Supporting Information for: Stochastic Simulation of Dopamine Neuromodulation for Implementation of Fluorescent Neurochemical Probes in the Striatal Extracellular Space

Abraham G. Beyene[1], Ian R. McFarlane[1], Rebecca Pinals[1], Markita P. Landry[1,2,3,*]
[1] Chemical and Biomolecular Engineering, University of California, Berkeley, CA 94720
[2] California Institute for Quantitative Biosciences, QB3, University of California, Berkeley, CA 94720
[3] Chan-Zuckerberg Biohub San Francisco, CA 94158

* landry@berkeley.edu

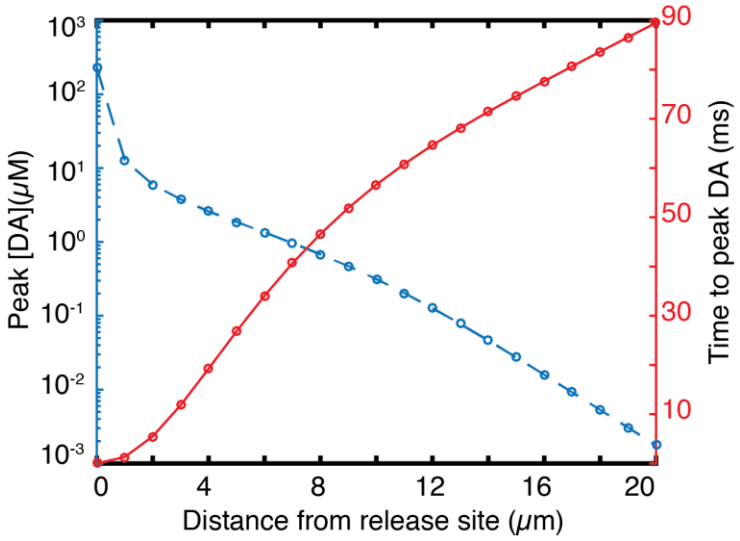

Figure S1. Peak dopamine concentration as a function of distance from release site following a single quantal release. Our simulation shows a peak dopamine concentration of 226µM at r = 0 µm (inside the synaptic cleft), which dissipates instantaneously as it expands out into the ECS. A peak dopamine concentration of 1 nM is observed at a distance of 20 µm from the release site with a diffusion-induced time delay of 90 ms from time of release.

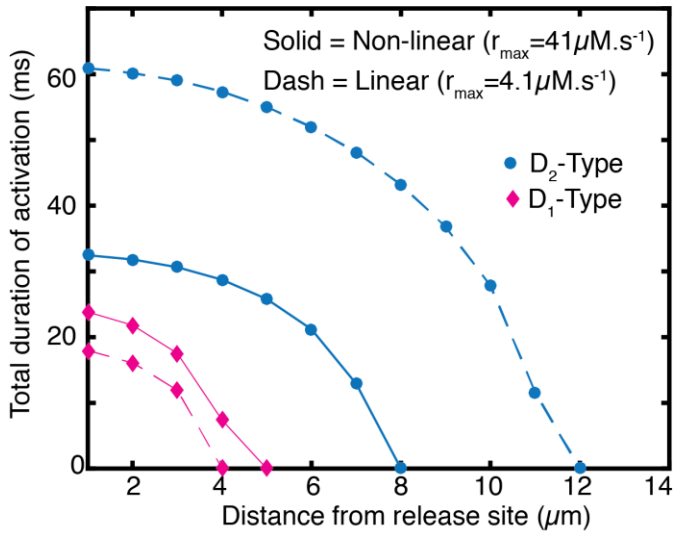

Figure S2. Comparison of non-linear dopamine reuptake versus linear uptake model. Non-linear dopamine reuptake with r_{max} at 41 µM.s^{-1} compared to linear uptake with r_{max} at 4.1 µM.s^{-1}. Both cases are run with an equal K_m of 0.21 µM. D_1 receptor activation shows similar behavior for both non-linear and linear reuptake. D_2 receptor activation with linear uptake underestimates extent of receptor activation when compared to non-linear reuptake modeling by one order of magnitude.

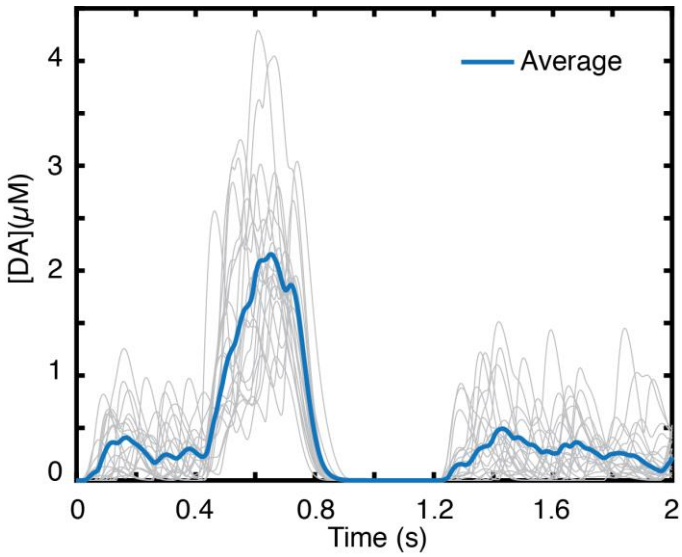

Figure S3. Averaging of multiple simulation runs for asynchronous terminal firing. Average (bold blue trace) of N=20 simulation runs (light gray traces) of 100 asynchronously firing terminals. The firing regime is as defined for Figure 4 of main manuscript and is omitted here for clarity.

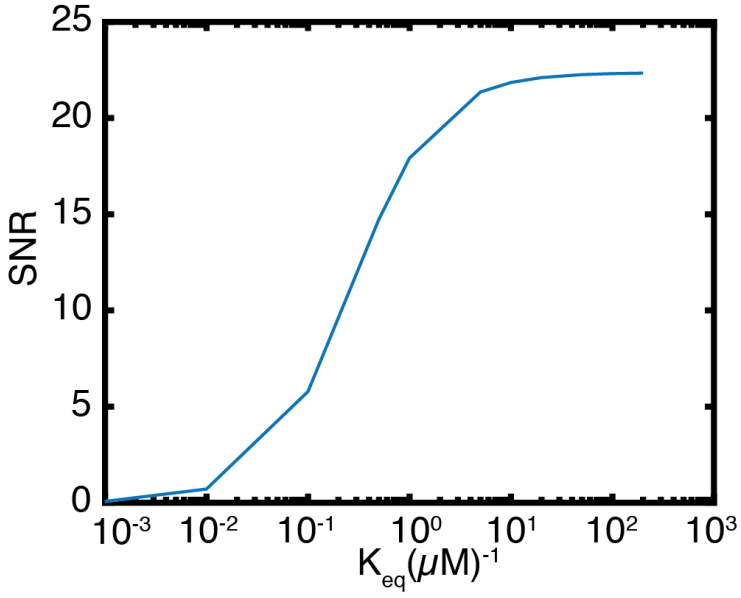

Figure S4. Dependence of SNR on the sensor parameter K_{eq}. High K_{eq} sensors have stronger turn-on response but poor reversibility. Imaging of faster dynamic processes, where temporal resolution is desired, require fast reversible sensors with low K_{eq} at a cost of lower SNR. Figure is developed for F_0 = 10,000 and imaging frame rate of 20 Hz.

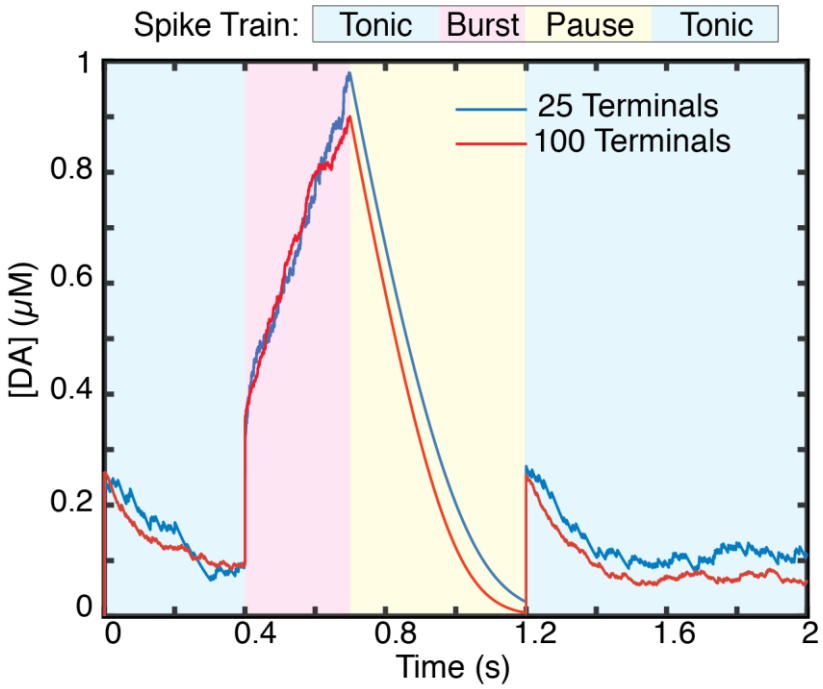

Figure S5. Volume-averaged behavior of 25 terminals vs. 100 terminals firing asynchronously. The result shows an average from N = 20 simulation runs for each 25- (blue) or 100- (red) terminal cluster. Volume-averaged dynamics shows behavior that is largely independent of cluster size for behavior-relevant firing regimes of burst firing and pause in firing. At smaller cluster sizes, the diffusive flux of dopamine out of the averaging volume becomes important and can no longer be ignored, resulting in slightly higher concentrations. For the 100 terminal cluster where release from a terminal does not escape the averaging volume size, accurate tonic and burst concentration levels can be estimated. Tonic dopamine level approaches 50 nM.

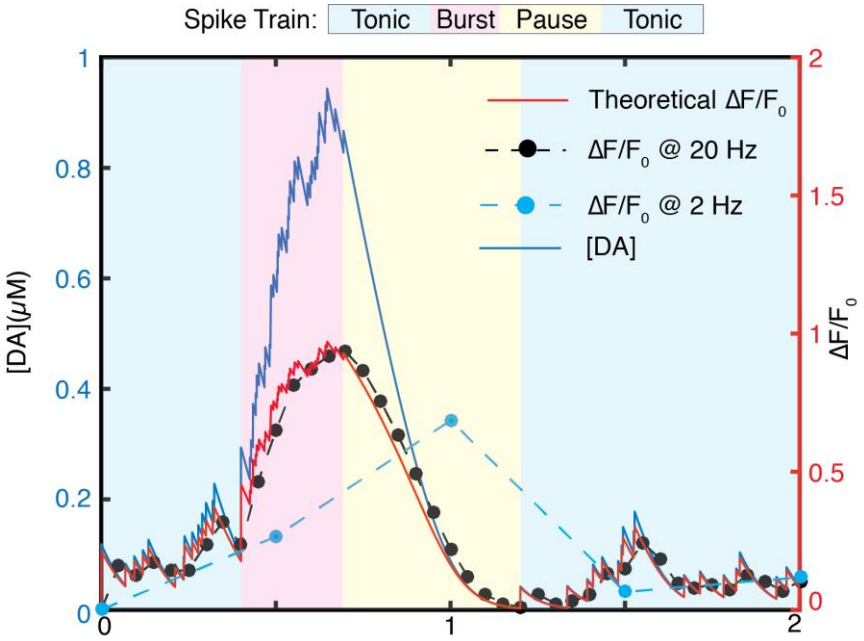

Figure S6 Volume-averaged behavior of 100 terminals firing asynchronously. Imaging at 2Hz fails to distinguish between behavior-relevant firing events of burst firing and pause in firing.

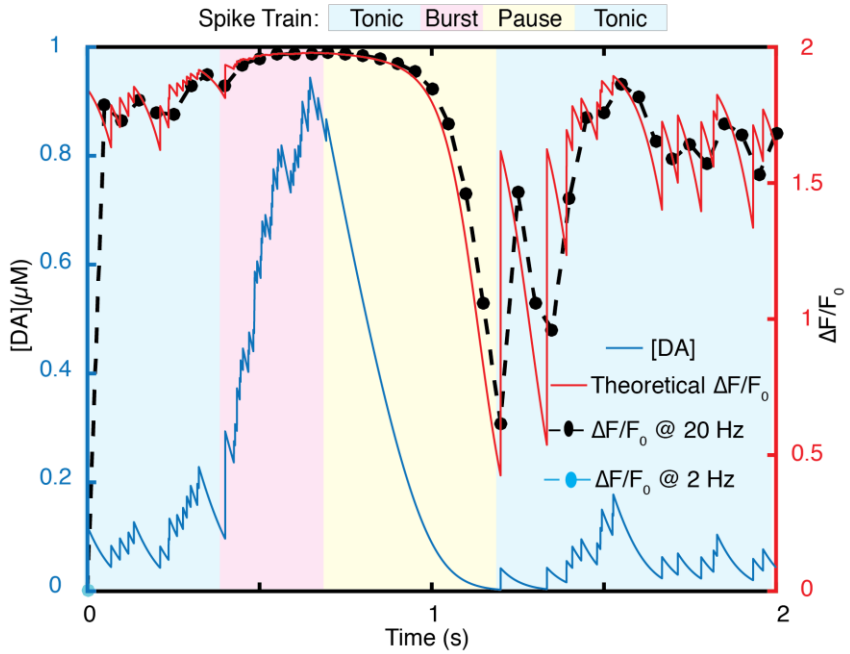

Figure S7. Volume average dynamics of 100 terminals firing asynchronously imaged with a sensor with K_{eq} = 100 μM^{-1}. The high nanosensor-analyte affinity results in nanosensor saturation at low (tonic) levels of dopamine.

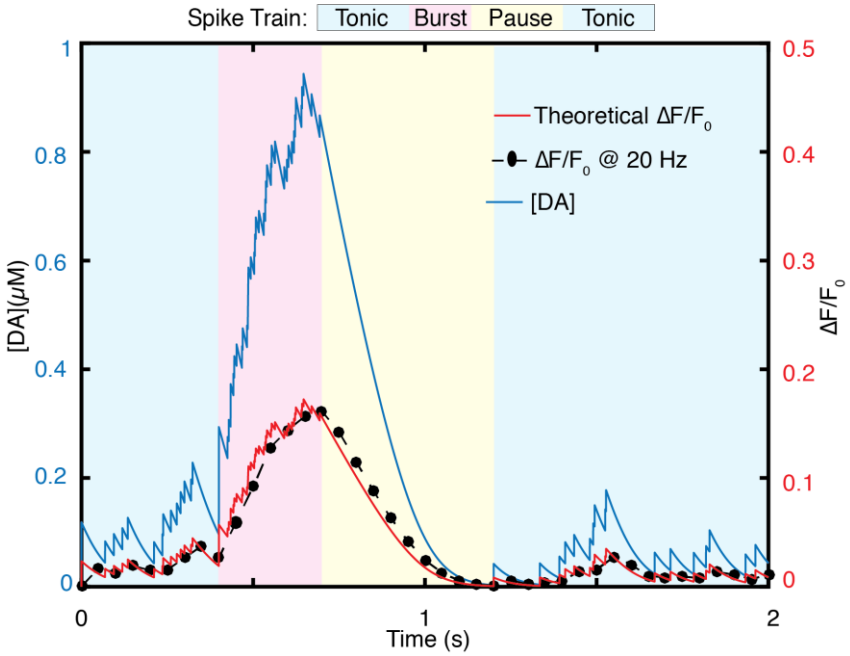

Figure S8. Volume average dynamics of 100 terminals firing asynchronously imaged with a sensor with K_{eq} = 0.1 μM^{-1}. The low nanosensor-analyte affinity results in decreased nanosensor sensitivity, with an exemplary burst firing event resulting in only 10% of the nanosensor peak $\Delta F/F_0$.